

Reducing roundoff errors in numerical integration of planetary ephemeris

Maksim Subbotin, Alexander Kodukov and Dmitry Pavlov

Faculty of Computer Science and Technology, St. Petersburg
Electrotechnical University, ul. Professora Popova 5,
St. Petersburg, 197022, Russian Federation.

*Corresponding author(s). E-mail(s): dapavlov@etu.ru;

Abstract

Modern lunar-planetary ephemerides are numerically integrated on the observational timespan of more than 100 years (with the last 20 years having very precise astrometrical data). On such long timespans, not only finite difference approximation errors, but also the accumulating arithmetic roundoff errors become important because they exceed random errors of high-precision range observables of Moon, Mars, and Mercury. One way to tackle this problem is using extended-precision arithmetics available on x86 processors. Noting the drawbacks of this approach, we propose an alternative: using double-double arithmetics where appropriate. This will allow to use only double precision floating-point primitives which have ubiquitous support.

Keywords: Numerical integration, floating-point arithmetics, N-body problem, planetary ephemeris.

1 Introduction

A lunar-planetary ephemeris is essentially a table that contains coordinates of Solar system planets and the Moon on a temporal grid. Lunar-planetary ephemerides are used for various purposes, including Earth and space navigation, prediction of orbits of asteroids and spacecraft, prediction of solar and lunar eclipses, and testing scientific hypotheses about fundamental properties of spacetime. Since 1960s, ephemerides are built on computers with numerical

routines integrating equation of motion. Modern lunar-planetary ephemerides (in order of first release) are: JPL DE [1], IAA EPM [2], INPOP IMCCE [3]. Also there exist ephemerides based on analytical theories instead of numerical integration, e. g. VSOP [4], but they are outside the scope of this work.

Equations of motion contain many free parameters that are determined from astrometrical observations. Throughout decades, the accuracy of ephemerides improved, following the improvement of the accuracy of the observations and improvement of mathematical models.

As a rule, the accuracy of a mathematical model must be the same or better than the accuracy of observations. In this work, we will be focusing on the orbits of three bodies with the most precise observations to date:

- The Moon — most precise lunar laser ranging normal points reach 1 mm accuracy [5, 6].
- Mars — most precise spacecraft radio ranging normal points reach 55 cm postfit rms [7].
- Mercury — MESSENGER spacecraft radio ranging normal points reach 60 cm postfit rms [2].

The problem we are dealing with in this work is the arithmetical roundoff errors that accumulate during the numerical integration of equations of motion, therefore affecting the accuracy of ephemeris.

2 Equations of motion

In this work, we use the dynamical model of EPM2021 ephemeris, though other ephemerides have similar dynamical models. The following bodies are included into the model:

- All planets;
- The Sun and the Moon;
- Pluto and 30 other transneptunian objects;
- 277 asteroids;
- Discrete uniform 180-point annulus approximating the asteroid belt;
- Discrete uniform 160-point ring approximating the Kuiper belt.

For details of how the bodies were chosen, we refer to [8–10]. Sixteen bodies (the Sun, the planets, Pluto, Ceres, Pallas, Vesta, Iris, Bamberga) obey Einstein–Infeld–Hoffmann equations of motion written up to $1/c^2$ terms:

$$\begin{aligned}
\mathbf{a}_i = & \sum_{j \neq i} \frac{Gm_j \mathbf{r}_{ij}}{r_{ij}^3} \\
& + \frac{1}{c^2} \sum_{j \neq i} \frac{Gm_j \mathbf{r}_{ij}}{r_{ij}^3} \left[v_i^2 + 2v_j^2 - 4(\mathbf{v}_i \mathbf{v}_j) - \frac{3(\mathbf{r}_{ji} \mathbf{v}_j)^2}{r_{ji}^2} \right. \\
& \quad \left. - 4 \sum_{k \neq i} \frac{Gm_k}{r_{ik}} - \sum_{k \neq j} \frac{Gm_k}{r_{jk}} + \frac{1}{2}(\mathbf{r}_{ij} \mathbf{a}_j) \right] \quad (1) \\
& + \frac{1}{c^2} \sum_{j \neq i} \frac{Gm_j}{r_{ij}^3} [\mathbf{r}_{ji}(4\mathbf{v}_i - 3\mathbf{v}_j)] (\mathbf{v}_i - \mathbf{v}_j) \\
& + \frac{7}{2c^2} \sum_{j \neq i} \frac{Gm_j \mathbf{a}_j}{r_{ij}}
\end{aligned}$$

where \mathbf{a} is acceleration; \mathbf{v} is velocity; Gm is the gravitational parameter; $\mathbf{r}_{ij} = \mathbf{r}_j - \mathbf{r}_i$ is the position of body j w.r.t. body i ; and c is the speed of light.

Note that the first term in Eq. (1) is Newtonian acceleration; also note that the accelerations are present also on the right hand side of Eq. (1), making it look as an implicit equation. However, in practice, the \mathbf{a}_j terms are replaced with Newtonian accelerations, which has negligible effect on the result.

Other point masses in the model interact with those 16 with only Newtonian forces and do not interact with each other. This compromise is made to speed up the calculations, with sub-centimeter impact on the orbits of the planets and sub-millimeter impact on the geocentric orbit of the Moon on the timespan of 40 years.

Other effects, important for dynamical model of ephemeris, were omitted in this study. Those are: accelerations from solar oblateness and Lense–Thirring effect; “point mass–figure” accelerations of the Earth that come from the Sun, Venus, Mars, Jupiter, and the Moon; the motion of the Moon as an elastic body with a rotating liquid core [11] experiencing tidal forces modeled with a delay differential equation [12].

The equations are numerically integrated with the step of 1/16 days with an Adams–Bashforth–Moulton multistep predictor-corrector scheme (PECEC mode) of order 13. The implementation used in this work was analogous to one described in [12], but without the “delay” part. The formulas of predictor and corrector are given in Eq. (2).

$$\begin{aligned}
\mathbf{x}_{n+1}^{(p)} &= \mathbf{x}_n + h \sum_{j=0}^{k-1} \gamma_j \nabla^j \mathbf{f}_n \\
\mathbf{x}_{n+1} &= \mathbf{x}_{n+1}^{(p)} + h \gamma_k \nabla^k \mathbf{f}_{n+1},
\end{aligned} \quad (2)$$

Here, \mathbf{x}_n is the state of the dynamical system, $\mathbf{f}_n = \mathbf{f}(\mathbf{x}_n)$ is the time derivative of \mathbf{x} , ∇ is the backward finite difference operator, h is the step size, n is the step number, k is the order of the method, and γ_j are precalculated coefficients.

4 *Reducing roundoff errors in numerical integration of planetary ephemeris*

For obtaining the $\mathbf{x}_2 \dots \mathbf{x}_k$, a single-step Dormand–Prince scheme of order 8 is used (with the step size of $h/8$).

The arithmetical roundoff errors happen in the numerical scheme itself as well as in the calculation of \mathbf{f} .

3 Estimation of numerical roundoff errors

3.1 Representation of numbers

The most common numerical data type in computers is IEEE 754 *double precision* — a 64-bit binary floating-point data type where the fractional part occupies 52 bits. Every number represented in this format is assumed to have an error which does not exceed half of the *unit in the last place* (ulp), i.e. the value of the last bit of the fractional part. For example, $1 + 2^{-52}$ is represented exactly in double precision, while anything between 1 and $1 + 2^{-53}$ is rounded down to 1, and anything between $1 + 2^{-53}$ and $1 + 2^{-52}$ is rounded up to $1 + 2^{-52}$. This gives the rough estimate of double precision representation being accurate to about $-\log_{10} 2^{-53} \approx 16$ decimal digits, and the relative error of representation of numbers hence being about 10^{-16} .

This is more than enough precision to represent astronomical data. For example, the maximum Earth–Moon distance is approximately 400000 km, while the best observations (see Sec. 1) have the accuracy of about 1 mm; so at any point in time, it makes sense to require the accuracy of the geocentric position of the Moon being 1 mm at best¹; that is, the relative error of representation of 2.5×10^{-12} will be enough.

Similarly, the maximum Earth–Mars distance is about 400 million km; to match the accuracy of observations of about 0.5 m, the relative error of 1.25×10^{-12} will be enough.

However, during the process of numerical integration, each arithmetical operation involving double precision numbers rounds its result to double precision again, and this roundoff error propagates to further calculations; as a result, the final orbits suffer from numerical errors that accumulate.

3.2 Two-way integration

In order to estimate the roundoff errors, one must find a way to separate them from approximation errors inherent to the numerical scheme and the errors in the underlying model. This is achieved via integration of the same equations forward and then backward over time. The backward integration uses the result of the forward integration as initial state. Mathematically, the two integrations should produce identical results. In reality, both integrations have model errors, approximation errors and numerical errors—but the errors

¹The semimajor axis of the orbit of the Moon in the ephemeris strongly correlates with X-coordinates of retroreflectors; hence, the said coordinates have the uncertainty of about 3 cm [13] at best. However, it still makes sense to require better accuracy in lunar ephemeris when geocentric coordinates of the retroreflectors are of interest; in those coordinates, the uncertainties of the X-coordinates of retroreflectors and the semimajor axis of the orbit of the Moon are largely canceled out.

of the first two kinds cancel out². The comparison of the orbits obtained with the two integrations thus gives us the estimate of the accumulated roundoff error. For previous usage of this technique, see e.g. [14].

In modern ephemeris, the initial parameters of orbits are determined from observations that cover the interval of about 100 years. The *epoch*—the date those parameters are referred to—is placed somewhere inside this interval, and the numerical integration is then performed in both directions from epoch. To reduce the overall error of the numerical integration, the epoch could be in the middle of the interval; but to account for the better precision of observations of modern times, the epoch is usually shifted right from the middle. In EPM, the epoch is Oct 27, 1984 (JD 2446000.5). In this work we will study the accumulation of roundoff error on the timespan of 40 years of integration (in one direction).

The roundoff errors of positions of Moon, Mercury, and Mars obtained with double precision and with the step size of 1/16 days are shown on Figs. 1–3. The one-way integration for 40 years took 81 seconds in this configuration. It is clear that the numerical roundoff errors from double precision are not below the accuracy of observations for all the three bodies: 25 cm for the Moon (normal points accuracy reach 1 mm), 2.5 m for Mercury (postfit rms of normal points reach 60 cm), and 70 cm for Mars (postfit rms of normal points reach 55 cm).

3.3 Barycenter

The (relativistic) barycenter of a system of N bodies is defined as follows:

$$\mathbf{b} = \frac{\sum_i \mu_i^* \mathbf{r}_i}{\sum_i \mu_i^*} \quad (3)$$

where μ_i^* is the body’s relativistic gravitational parameter:

$$\mu_i^* = \mu_i \left(1 + \frac{1}{2c^2} \dot{r}_i^2 - \frac{1}{2c^2} \sum_{j \neq i} \frac{\mu_j}{r_{ij}} \right) \quad (4)$$

Initial positions and velocities of the bodies are equally adjusted so that the position of the barycenter and the momentum are zero:

$$\begin{cases} \sum_i \mu_i^* \mathbf{r}_i = \mathbf{0} \\ \sum_i \mu_i^* \dot{\mathbf{r}}_i = \mathbf{0} \end{cases} \quad (5)$$

Mathematically, the barycenter of the system should stay in the origin throughout the integration, but errors of approximation and numerical roundoff cause it to drift. On Fig. 4, we examine the distance from the barycenter to the origin (as function of time) as an additional consistency check of the

²In a multistep scheme, the approximations are slightly different near the ends of the timespan of integration due to the “warm-up” stage, but as we will later see, this difference does not make any noticeable impact.

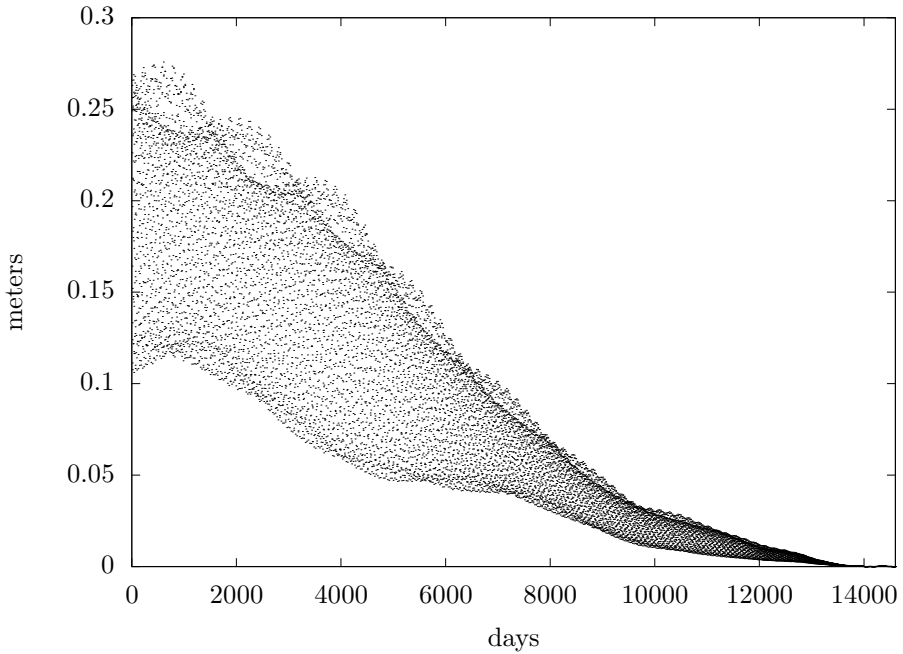


Fig. 1 The roundoff errors of positions of Moon with double precision. Hereinafter, the position of the Moon is implied geocentric, while the positions of planets are barycentric.

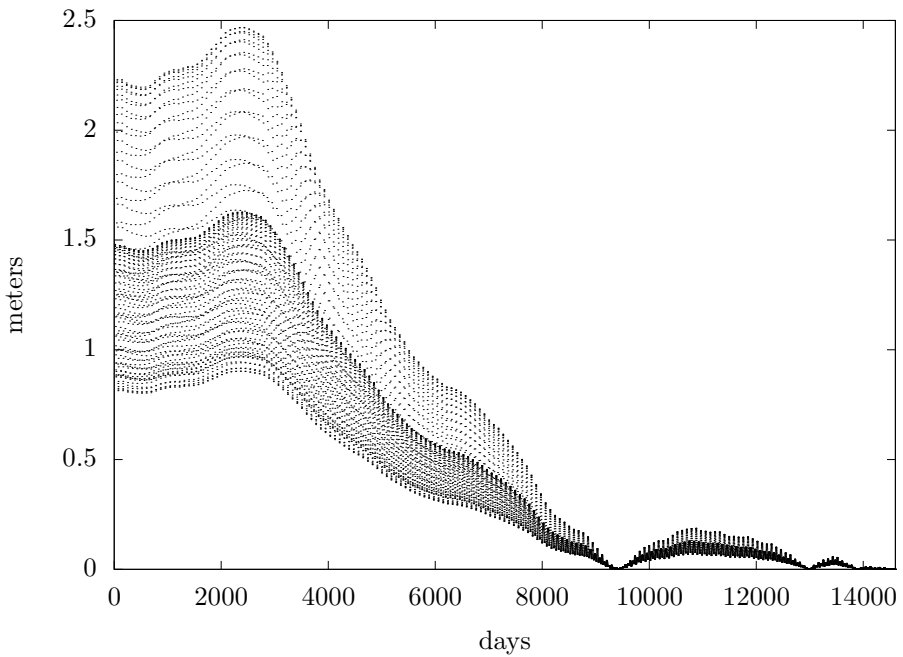


Fig. 2 The roundoff errors of positions of Mercury with double precision

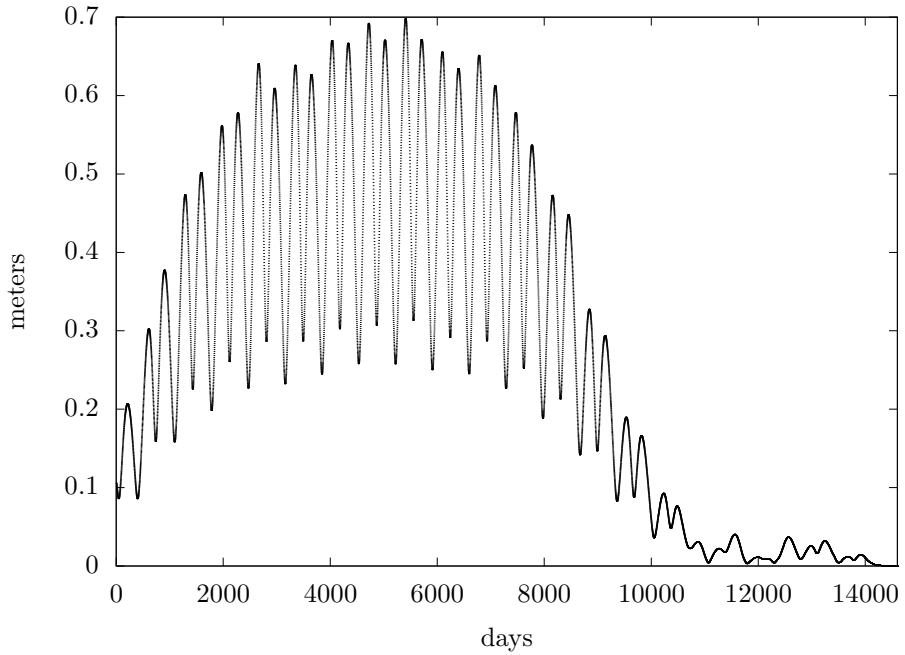


Fig. 3 The roundoff errors of positions of Mars with double precision

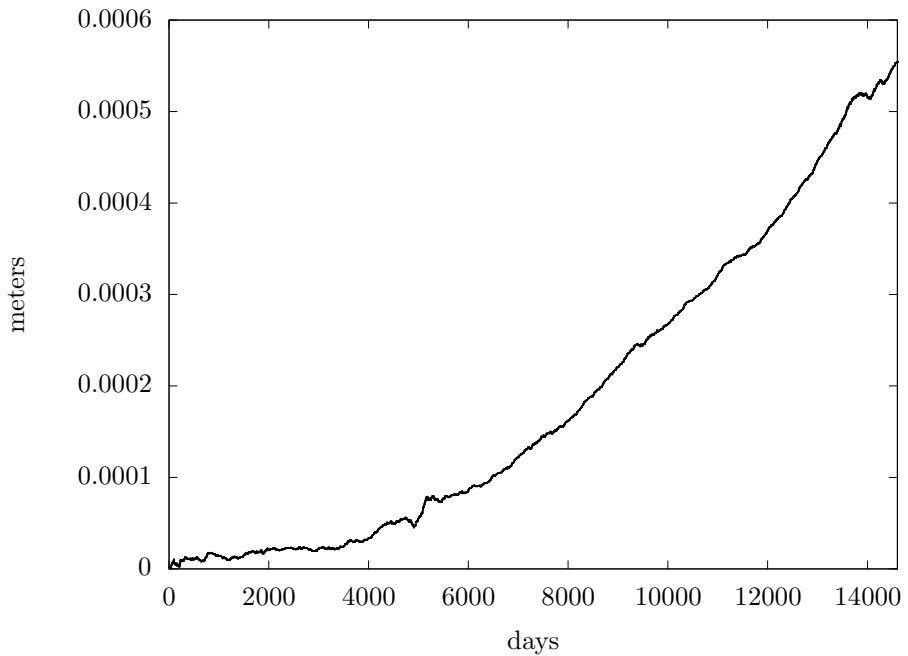


Fig. 4 Drift of barycenter with double precision

correctness of the implementation of the EIH equations (1) and the correctness and stability of the difference scheme (2). The sub-millimeter value of the drift confirms that the consistency check is passed.

4 Reducing the roundoff errors

4.1 Existing approaches

All mitigations of the problem of accumulating roundoff errors are based, in one way or another, on using data types other than double precision. DE ephemerides prior to DE405 (1997) were integrated on a UNIVAC mainframe using its native 72-bit floating-point type with 60-bit fraction (coincidentally, that type was also called double precision); DE405 was integrated on VAX Alpha using its native 128-bit floating-point type with 112-bit fraction, *quadruple precision* [15]. DE410 (2003) was integrated on Sun Ultra with an UltraSPARC processor using ordinary double precision, which caused the problems with numerical noise, limiting accuracy of orbits at 1–2 meters [16]. The numerical integrator with which DE was built was called DIVA [17]. By the time of DE414 (2006), DIVA was upgraded to QIVA, where “Q” stands for quadruple precision (not implemented in hardware, but emulated by Fortran compiler). In fact, a mixed mode was used: only the newtonian part of acceleration was computed in quadruple precision, while all the remaining perturbations were computed in double precision. Still, the mixed mode required 30x more time than double precision mode. QIVA is probably used to build DE ephemerides to this day, though compilers might since have improved their emulation. It is important to note that quadruple precision is very excessive for the task.

All public versions of EPM since EPM2004, as well as all versions of INPOP since INPOP06, were numerically integrated with 80-bit *extended precision* type (63-bit fraction). This precision is enough for planetary orbits, see Figs. 5–8. However, it has its own drawbacks:

- Extended precision is supported exclusively on x86 architecture (Intel and AMD processors), but not on ARM-based processors which seem to be gaining significant share (Apple M1, Microsoft SQ1, AWS Graviton, almost all mobile chips).
- Few programming languages provide support extended precision, namely Delphi, C/C++, D, Perl, Racket BC³, Swift, and some implementations of Common Lisp and Fortran. Extended precision in Fortran is limited to gfortran compiler; Intel and Absoft Fortran compilers do not support it.
- While simple operations with extended precision numbers are as fast as operations with double precision numbers in x86, SIMD extensions of x86 architecture (MMX, SSE, AVX, AVX-512) are not available for extended

³“BC” stands for “before Chez”, the Racket compiler and virtual machine that existed before they were replaced with Chez Scheme, but are still supported.

precision numbers. This limitation causes 4x slowdown from double precision mode. (The integration in one direction for 40 years took 323 seconds.)

4.2 Implementation of double-double arithmetic

Double-double arithmetic is a software method to increase floating-point precision that uses pairs of double precision values to store numbers and performs arithmetic operation basing on arithmetics with double precision. Double-double numbers are defined as the unevaluated sums of two double components (larger and smaller part): $x = x_{\text{low}} + x_{\text{high}}$, $|x_{\text{low}}| \leq 0.5 \cdot \text{ulp}(x_{\text{high}})$ so their significands don't overlap. Such technique allows to store numbers with significands of at least $2 \cdot 53 = 106$ bits.

Double-double arithmetic does not require special hardware nor programming language support (software implementation [18] is available). The algorithms of some basic operations for the double-double type are shown below.

- Dekker's summation of two double precision numbers with error [19]. $\text{RN}(x)$ means rounding to nearest.

Algorithm 1 Fast2Sum (a, b), $a \geq b$

```

s ← RN(a + b)
z ← RN(s - a)
t ← RN(b - z)
return (s, t)

```

- Dekker's double-double summation [19]. The Fast2Sum algorithm is used to add up the large components and then to add the summation error to small components.

Algorithm 2 DDSum (x_h, x_l, y_h, y_l)

```

if  $|x_h| \geq |y_h|$  then
  ( $r_h, r_l$ ) ← Fast2Sum( $x_h, y_h$ )
   $s \leftarrow \text{RN}(\text{RN}(r_l + y_l) + x_l)$ 
else
  ( $r_h, r_l$ ) ← Fast2Sum( $y_h, x_h$ )
   $s \leftarrow \text{RN}(\text{RN}(r_l + x_l) + y_l)$ 
end if
return Fast2Sum( $r_h, s$ )

```

- Double multiplication with error (uses *fused multiply-add* instruction, or FMA).

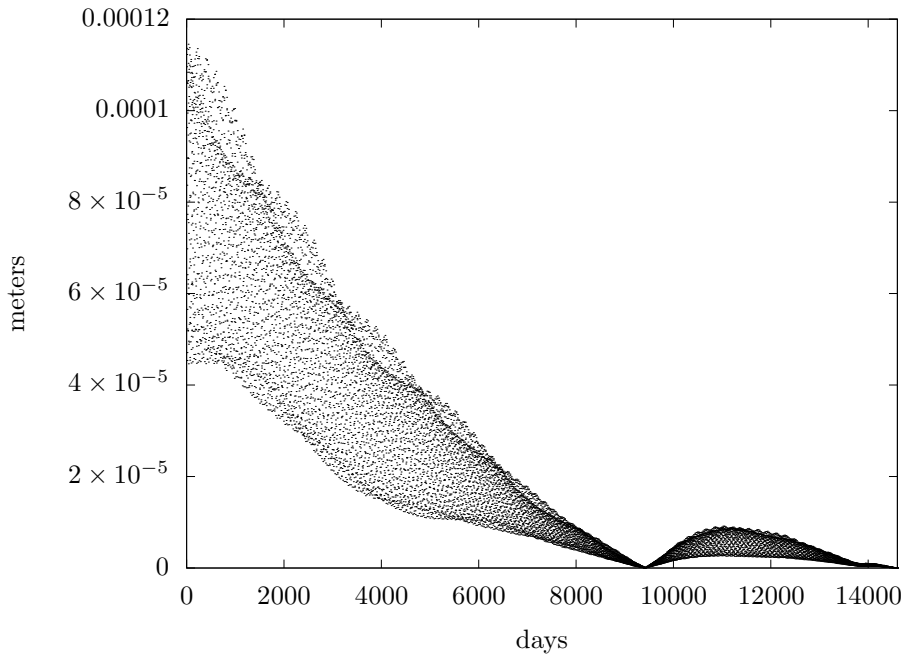


Fig. 5 The roundoff errors of the position of the Moon with extended precision

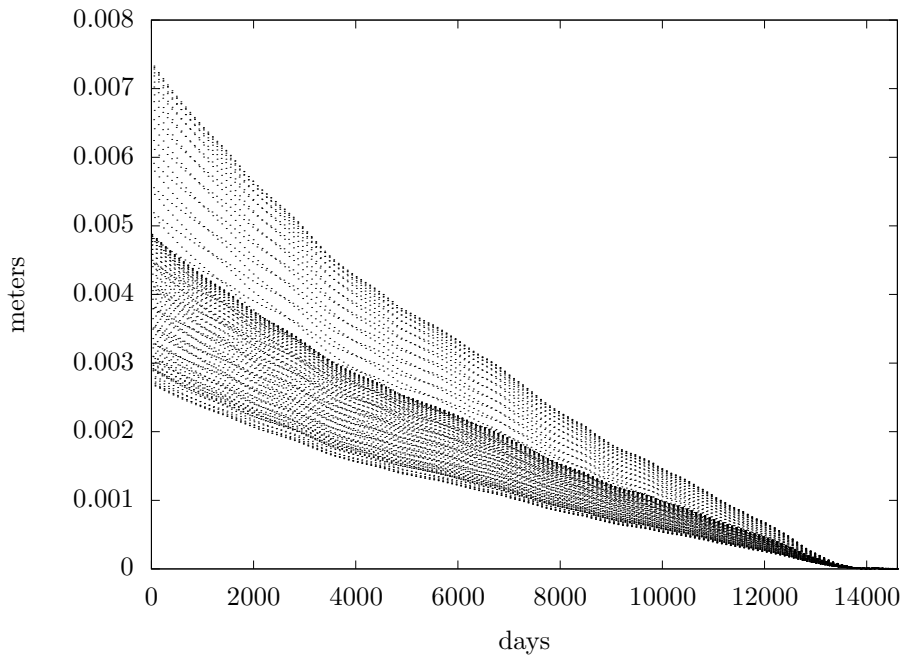


Fig. 6 The roundoff errors of the position of Mercury with extended precision

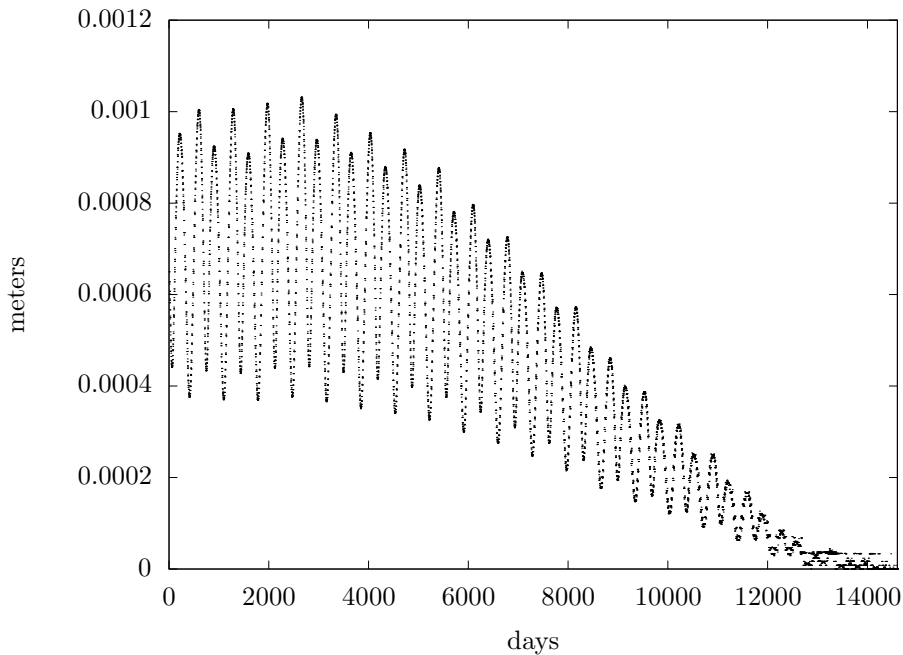


Fig. 7 The roundoff errors of the position of Mars with extended precision

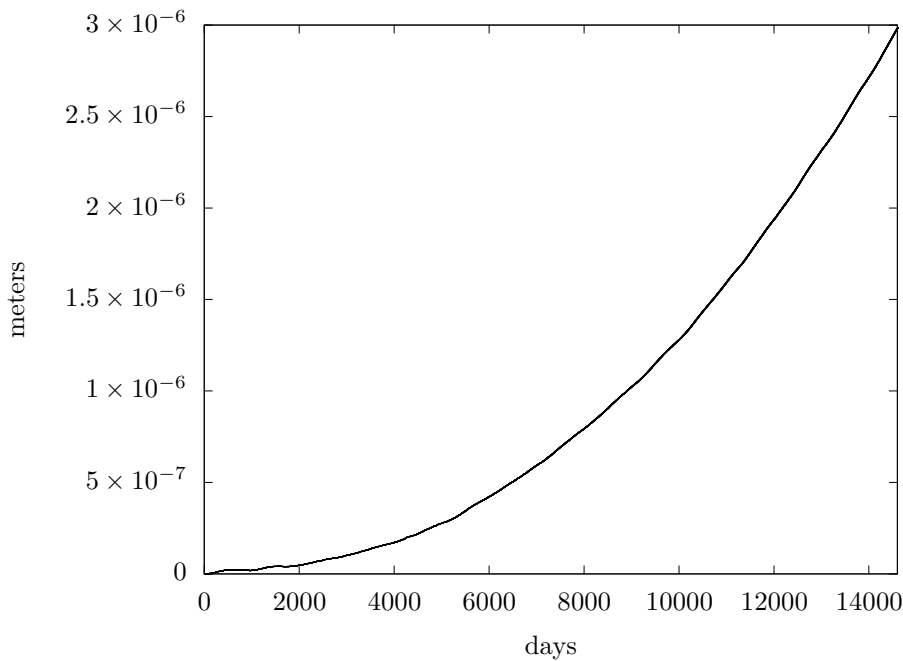


Fig. 8 Drift of barycenter with extended precision

Algorithm 3 Product(x, y)

```

 $p \leftarrow x \cdot y$ 
 $e \leftarrow \text{FMA}(x, y, -p)$ 
return ( $p, e$ )

```

- Double-double multiplication [19].

Algorithm 4 DDProduct (x_h, x_l, y_h, y_l)

```

( $c_h, c_l$ )  $\leftarrow$  Product( $x_h, y_h$ )
 $p_1 \leftarrow \text{RN}(x_h \cdot y_l)$ 
 $p_2 \leftarrow \text{RN}(x_l \cdot y_h)$ 
 $c_l \leftarrow \text{RN}(c_l + \text{RN}(p_1 + p_2))$ 
return Fast2Sum( $c_h, c_l$ )

```

- Double-double division [18]. The first approximation is $q_0 = x_h/y_h$. The remainder is $r = x - q_0 \cdot y$. The correction term is $q_1 = r_h/b_h$. Finally, Fast2Sum(q_0, q_1) renormalizes the result. TwoOneProd is the product of double-double and double (written similarly to DDProduct). 2Sum is the summation for cases where order of arguments for Fast2Sum is unknown.

Algorithm 5 DDDiv (x_h, x_l, y_h, y_l)

```

 $t_h \leftarrow \text{RN}(x_h/y_h)$ 
( $r_h, r_l$ )  $\leftarrow$  TwoOneProd( $y_h, y_l, t_h$ )
( $\pi_h, \pi_l$ )  $\leftarrow$  2Sum( $x_h, -r_h$ )
 $\sigma_h \leftarrow \text{RN}(\pi_l - r_l)$ 
 $\sigma_l \leftarrow \text{RN}(\sigma_h + x_l)$ 
 $\sigma \leftarrow \text{RN}(\pi_h + \sigma_l)$ 
 $t_l \leftarrow \text{RN}(\sigma/y_h)$ 
return Fast2Sum( $t_h, t_l$ )

```

- Double-double square root. The QD library [18] uses Karp's trick for square root [20]. If s is approximation for \sqrt{x} (QD uses $\sqrt{x_h}$), then $\sqrt{x} \approx x \cdot s + [x - (x \cdot s)^2] \cdot s/2$.

As part of the experiment, a full double-double implementation of the numerical integrator was done in this work. The results can be seen on Figs. 9–12. Clearly, the numerical roundoff errors are negligible, but this comes at great performance cost: the one-way integration for 40 years took 32 minutes, which is a 24x slowdown from double precision.

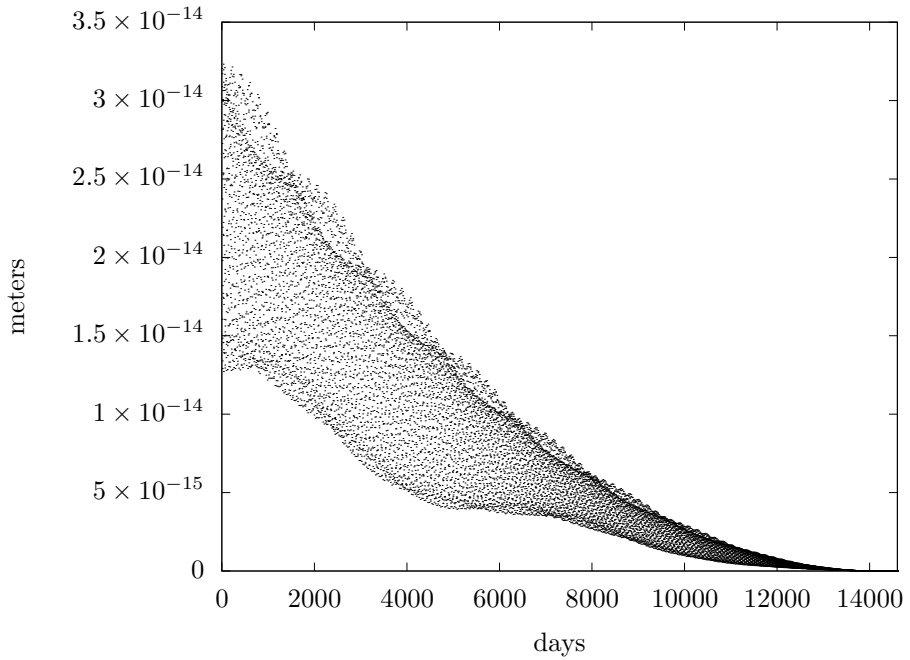


Fig. 9 The roundoff errors of the position of the Moon with double-double precision

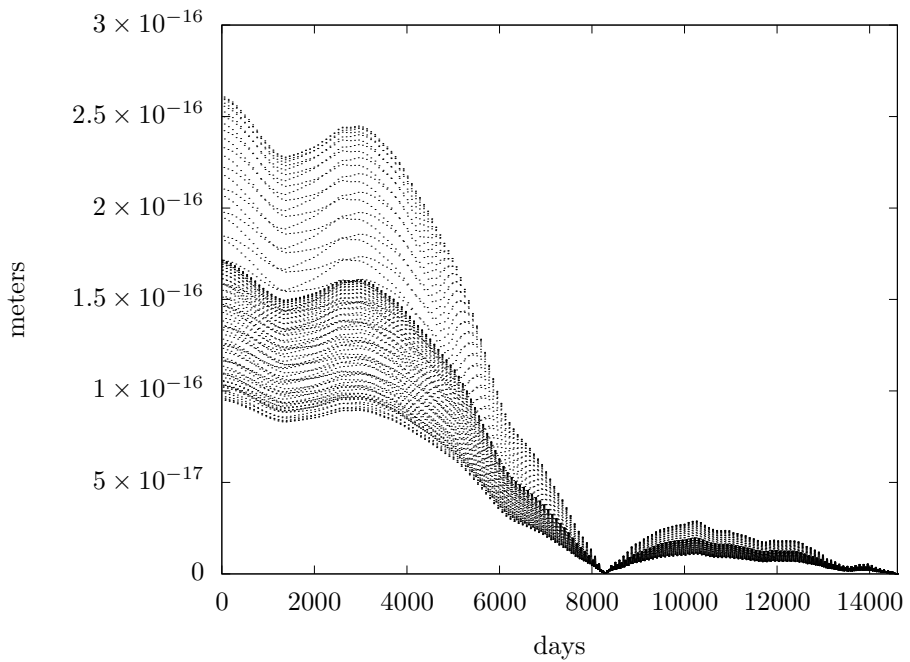


Fig. 10 The roundoff errors of the position of Mercury with double-double precision

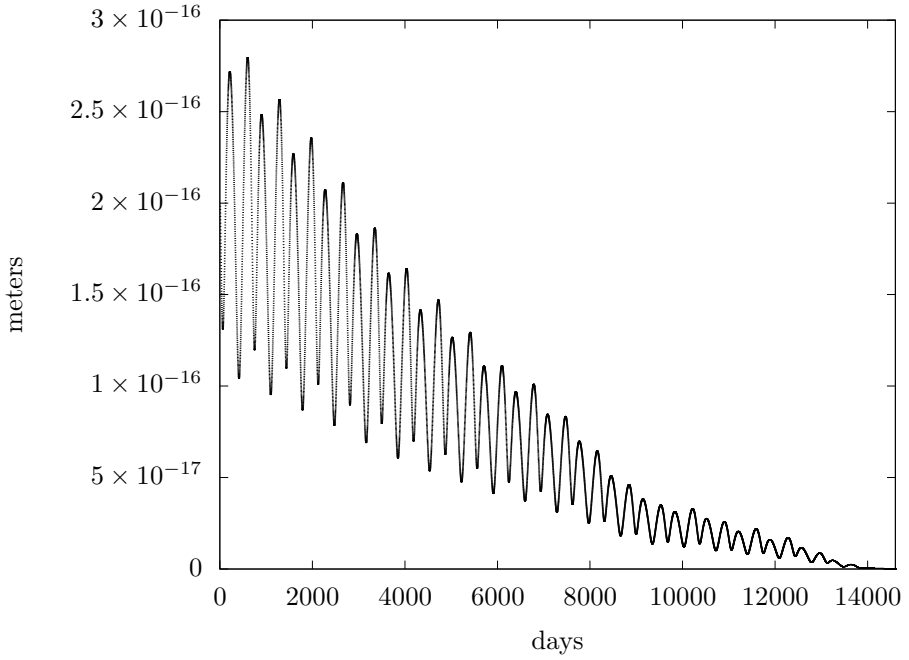


Fig. 11 The roundoff errors of the position of Mars with double-double precision

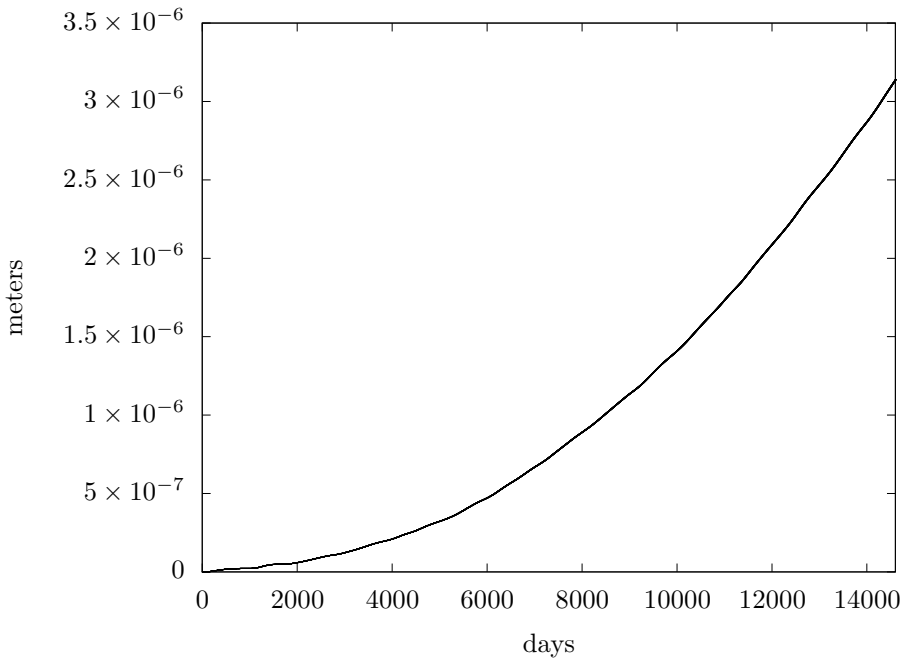


Fig. 12 Drift of barycenter with double-double precision

4.3 Selective usage of double-double types

By trial and error, the following scheme was worked out to maintain the balance between the precision and performance of calculations:

- The state of the system \mathbf{x} and its time derivative \mathbf{f} are stored in double-double precision, as well as the intermediate values in the PECEC scheme.
- The finite differences ∇^i are stored in double precision. However, the coefficients γ_i are stored in double-double precision.
- In the calculation of $\mathbf{f}(\mathbf{x})$, i.e. in Eq. (1), the \mathbf{r}_{ij} vectors and r_{ij} distances are stored in double precision.
- In the relativistic part of Eq. (1), \mathbf{v}_i and \mathbf{a}_i are rounded down to double precision, and all calculations are performed in double precision.
- The constant $1/c^2$ and the gravitational parameters Gm_i are also stored in double precision.

4.4 Special treatment of the Earth–Moon system

Let us denote $\mathbf{r}_{EM} = \mathbf{r}_M - \mathbf{r}_E$ the Earth–Moon vector. All \mathbf{r}_i in Eq. (1) are supposed to be referred to a single inertial frame (barycentric celestial reference system, or BCRS, in our case). However, a direct calculation of $\mathbf{r}_M - \mathbf{r}_E$ will result in a value that is about 400 times smaller than the subtrahend and the minuend, thus causing the loss of precision from the “catastrophic cancellation” of significant bits. This is particularly unwanted for \mathbf{r}_{EM} because of the high requirements to the numerical accuracy of the Moon’s orbit. In all three families of ephemerides (DE, EPM, INPOP) the orbit of the Moon is integrated in geocenter, so that \mathbf{r}_{EM} enters \mathbf{x} while the barycentric \mathbf{r}_M is temporarily restored during the calculation of \mathbf{f} .

Similarly, we aim to avoid the catastrophic cancellation in the calculation of the Newtonian acceleration of the geocentric Moon. For mutual Newtonian forces between Earth and Moon, this is rather simple. In Eq. (6), no subtraction of close numbers is involved.

$$\mathbf{a}_{EM}^{(E,M)} = \mathbf{a}_M^{(E)} - \mathbf{a}_E^{(M)} = -\frac{Gm_M + Gm_E}{r_{EM}^3} \mathbf{r}_{EM} \quad (6)$$

For geocentric Moon acceleration exerted by other bodies, we can apply a Taylor expansion. For body A, we aim to avoid direct subtraction of the Newtonian accelerations of the Moon $\mathbf{a}_M^{(A)}$ and Earth $\mathbf{a}_E^{(A)}$ caused by this body:

$$\begin{aligned} \mathbf{a}_{EM}^{(A)} &= \mathbf{a}_M^{(A)} - \mathbf{a}_E^{(A)} = Gm_A \left(\frac{\mathbf{r}_{MA}}{r_{MA}^3} - \frac{\mathbf{r}_{EA}}{r_{EA}^3} \right) \\ &= \frac{Gm_A}{r_{MA}^3} \left[\mathbf{r}_{MA} - \mathbf{r}_{EA} \left(\frac{(\mathbf{r}_{EA} - \mathbf{r}_{EM})^2}{r_{EA}^2} \right)^{3/2} \right] \\ &= \frac{Gm_A}{r_{MA}^3} \left[\mathbf{r}_{MA} - \mathbf{r}_{EA} \left(1 - 2 \frac{\mathbf{r}_{EA} \mathbf{r}_{EM}}{r_{EA}^2} + \frac{r_{EM}^2}{r_{EA}^2} \right)^{3/2} \right] \end{aligned} \quad (7)$$

Precision	double	extended	mixed	double-double
Max. error for Moon	0.28 m	0.1 mm	1.2 mm	$3.2 \cdot 10^{-14}$ m
Max. error for Mercury	2.47 m	7 mm	8.4 mm	$2.6 \cdot 10^{-16}$ m
Max. error for Mars	0.7 m	1 mm	0.44 mm	$2.8 \cdot 10^{-16}$ m
Max. drift of barycenter	0.5 mm	2.9 μ m	2.6 μ m	3.14 μ m
Time of integration	81 s	323 s	246 s	32 min

Table 1 Comparative results for 40 years of numerical integration with different data types.

Denoting $x = 2 \frac{r_{EA} r_{EM}}{r_{EA}^2} - \frac{r_{EM}^2}{r_{EA}^2}$ and applying the Taylor expansion of $(1 - x)^{3/2}$, we get

$$\mathbf{a}_{EM}^{(A)} \approx \frac{Gm_A}{r_{MA}^3} \left[-\mathbf{r}_{EM} - \mathbf{r}_{EA} \left(-\frac{3x}{2} + \frac{3x^2}{8} + \frac{x^3}{16} + \frac{3x^4}{128} \right) \right] \quad (8)$$

in which there is no subtraction of close values. Also, it was found out that double precision is enough for Eq. (8) and that four terms of Taylor expansion are required, but not more.

4.5 Results

The final results obtained with the mixed precision approach (Sec. 4.3) and with the special treatment of the Earth–Moon system (Sec. 4.4) are shown of Figs. 13–16. The accuracy is comparable to that obtained with extended precision. The one-way integration for 40 years took 246 seconds.

5 Conclusion

We summarize the results in Table 1. It can be clearly seen that the integration in “mixed” mode developed in this work gives the numerical roundoff errors that are small enough for the modern ephemeris astronomy, while not requiring any primitive datatypes other than the 64-bit double precision.

The “mixed” mode is just 3 times slower than the double precision mode and 1.3 times faster than the extended precision mode. The latter can be explained by the fact that the extended precision does not enjoy SIMD extensions in x86 hardware.

It must be noted that the results of such measurements are generally affected by the equations used (the number of asteroids and other point masses, figure effects, etc). The figure effects are particularly important for the orbital and rotational motion of the Moon. Also, derivatives of \mathbf{x} w.r.t. model parameters are often integrated alongside the dynamical equations. All this additional complexity was omitted in this work; however, it is not likely to change the results in principle. Equations of the rotation of the Moon can be easily implemented in double-double without significant impact on overall performance; figure effects in acceleration are small enough to be computed in double precision; and for the derivatives, high precision is not required.

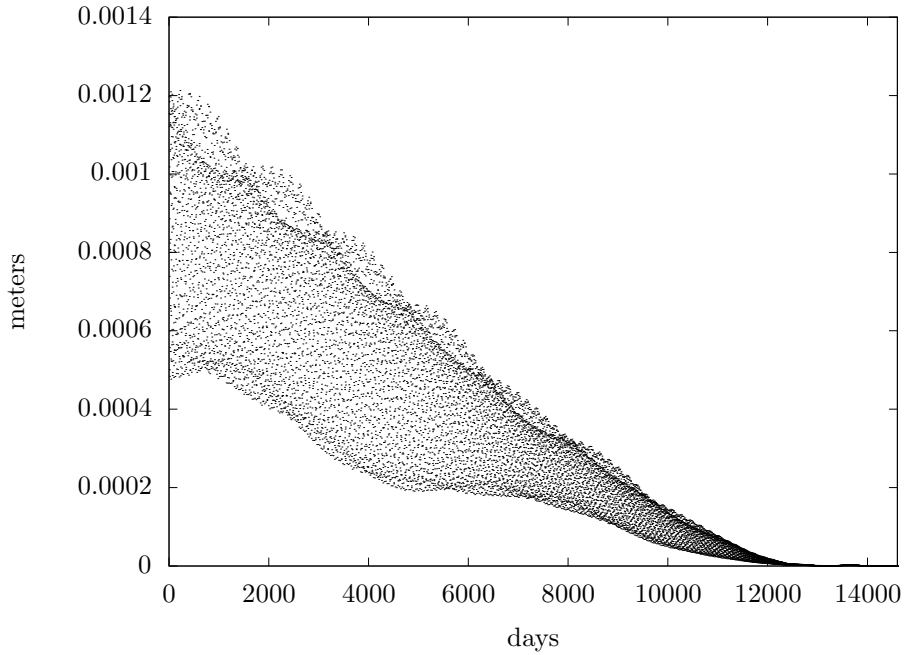


Fig. 13 The roundoff errors of the position of the Moon with mixed precision

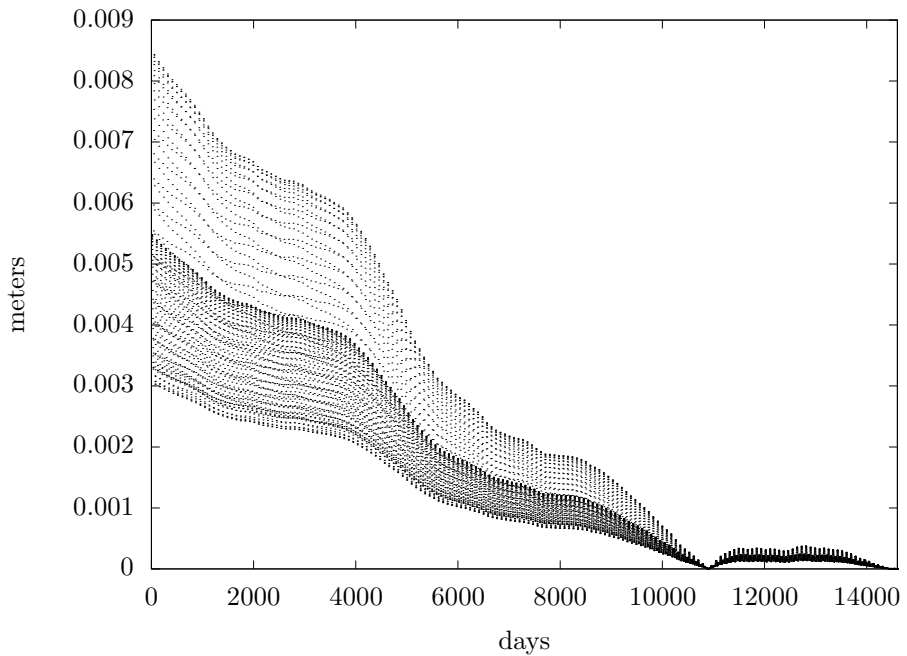


Fig. 14 The roundoff errors of the position of Mercury with mixed precision

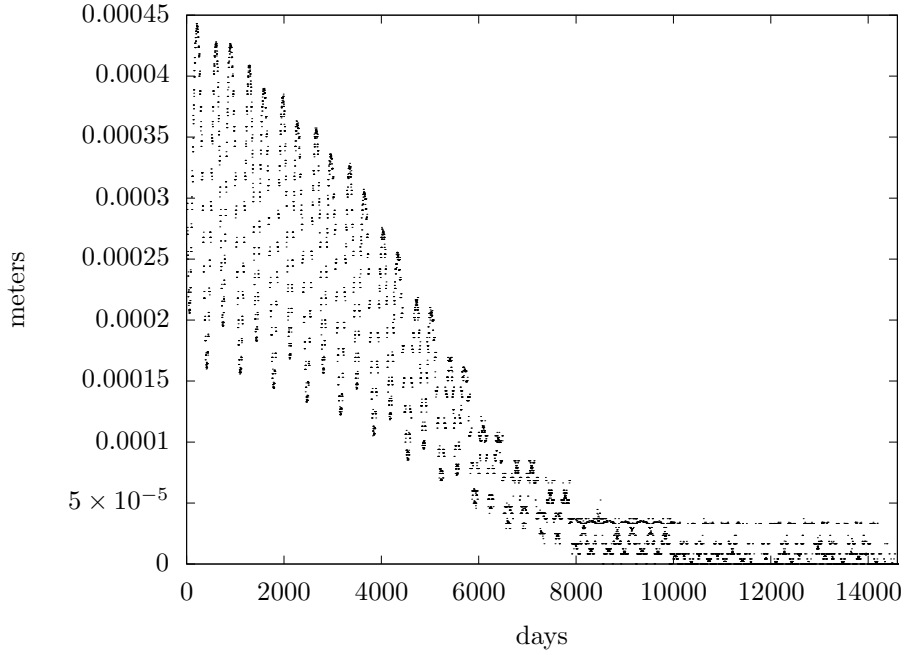


Fig. 15 The roundoff errors of the position of Mars with mixed precision

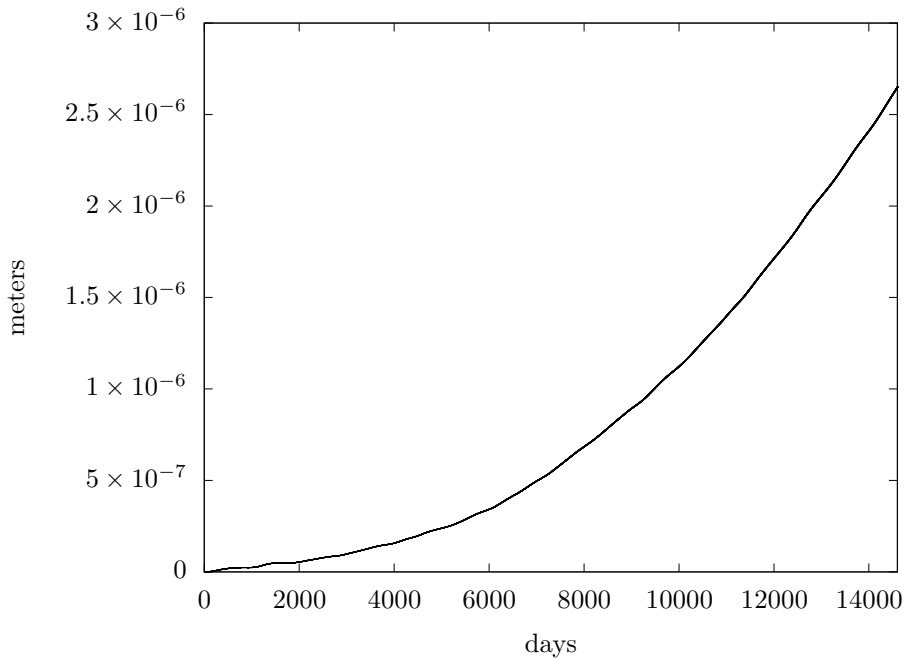


Fig. 16 Drift of barycenter with mixed precision

Data availability

The program code and data used for numerical integration in this work are available online: <https://github.com/S1ckick/Nbodies>.

References

- [1] Park, R.S., Folkner, W.M., Williams, J.G., Boggs, D.H.: The JPL planetary and lunar ephemerides DE440 and DE441. *The Astronomical Journal* **161**(3), 105 (2021). <https://doi.org/10.3847/1538-3881/abd414>
- [2] Pitjeva, E., Pavlov, D., Aksim, D., Kan, M.: Planetary and lunar ephemeris EPM2021 and its significance for solar system research. *Proceedings of the International Astronomical Union* **15**(S364), 220–225 (2022). <https://doi.org/10.1017/S1743921321001447>
- [3] Fienga, A., Deram, P., Di Ruscio, A., Viswanathan, V., Camargo, J.I.B., Bernus, L., Gastineau, M., Laskar, J.: INPOP21a planetary ephemerides. *Notes Scientifiques et Techniques de l'Institut de Mécanique Céleste, S110, Observatoire de Paris* (2021). <https://www.imcce.fr/content/medias/recherche/equipes/asd/inpop/inpop21a.pdf>
- [4] Simon, J.-L., Francou, G., Fienga, A., Manche, H.: New analytical planetary theories VSOP2013 and TOP2013. *A&A* **557**, 49 (2013). <https://doi.org/10.1051/0004-6361/201321843>
- [5] Murphy, T.W., Adelberger, E.G., Battat, J.B.R., Hoyle, C.D., Johnson, N.H., McMillan, R.J., Stubbs, C.W., Swanson, H.E.: APOLLO: millimeter lunar laser ranging. *Classical and Quantum Gravity* **29**(18), 184005 (2012). <https://doi.org/10.1088/0264-9381/29/18/184005>
- [6] Courde, C., Torre, J. M., Samain, E., Martinot-Lagarde, G., Aimar, M., Albanese, D., Exertier, P., Fienga, A., Mariey, H., Metris, G., Viot, H., Viswanathan, V.: Lunar laser ranging in infrared at the Grasse laser station. *A&A* **602**, 90 (2017). <https://doi.org/10.1051/0004-6361/201628590>
- [7] Kuchynka, P., Folkner, W.M., Konopliv, A.S.: Station-Specific Errors in Mars Ranging Measurements. *Interplanetary Network Progress Report 42-190, NASA JPL* (2012). https://ipnpr.jpl.nasa.gov/progress_report/42-190/190C.pdf
- [8] Pitjeva, E.V., Pitjev, N.P.: Masses of the main asteroid belt and the kuiper belt from the motions of planets and spacecraft. *Astronomy Letters* **44**(8-9), 554–566 (2018). <https://doi.org/10.1134/s1063773718090050>
- [9] Pitjeva, E.V., Pitjev, N.P.: Mass of the Kuiper belt. *Celestial Mechanics*

- and Dynamical Astronomy **130**(9), 57 (2018). <https://doi.org/10.1007/s10569-018-9853-5>
- [10] Kan, M., Pavlov, D.: Dynamical estimation of masses of the Main Asteroid Belt and some individual asteroids within the EPM ephemeris using infrared data. In: Astronomy at the Epoch of Multimessenger Studies. Proceedings of the VAK-2021 Conference, pp. 93–95. SAI MSU, INASAN, Moscow (2022). https://www.vak2021.ru/wp-content/uploads/2022/03/VAK_2021_proceedings.pdf
- [11] Pavlov, D., Williams, J., Suvorkin, V.: Determining parameters of Moon’s orbital and rotational motion from LLR observations using GRAIL and IERS-recommended models. *Celestial Mechanics and Dynamical Astronomy* **126**(1), 61–88 (2016). <https://doi.org/10.1007/s10569-016-9712-1>
- [12] Aksim, D., Pavlov, D.: On the extension of Adams–Bashforth–Moulton Methods for numerical integration of delay differential equations and application to the Moon’s orbit. *Mathematics in Computer Science* **14**, 103–109 (2020). <https://doi.org/10.1007/s11786-019-00447-y>
- [13] Pavlov, D.: Role of lunar laser ranging in realization of terrestrial, lunar, and ephemeris reference frames. *Journal of Geodesy* **94**(1) (2019). <https://doi.org/10.1007/s00190-019-01333-y>
- [14] Fienga, A., Manche, H., Laskar, J., Gastineau, M.: INPOP06: a new numerical planetary ephemeris. *A&A* **477**(1), 315–327 (2008). <https://doi.org/10.1051/0004-6361/20066607>
- [15] Standish E. M., Newhall X. X., Williams J. G., Yeomans D. K.: In: Seidelmann P. K. (ed.) *Orbital Ephemerides of the Sun, Moon, and Planets*, pp. 279–374. University Science Books, Herndon, VA (1992). <https://ssd.jpl.nasa.gov/ftp/eph/planets/ioms/ExplSupplChap8.pdf>
- [16] Standish, E.M.: JPL Planetary Ephemeris DE410. Jet Propulsion Laboratory Interoffice Memorandum 312.N–03–009, California Institute of Technology (2003). <https://ssd.jpl.nasa.gov/ftp/eph/planets/ioms/de410.iom.pdf>
- [17] Krogh, F.T.: An Adams Guy Does the Runge-Kutta. Section 395. Computing Memorandum 554., California Institute of Technology (1997). <https://trs.jpl.nasa.gov/bitstream/handle/2014/22564/97-1071.pdf>
- [18] Hida, Y., Li, S., Bailey, D.: Library for double-double and quad-double arithmetic. Technical report, Lawrence Berkeley National Laboratory (2008). <https://www.davidhbailey.com/dhbpapers/qd.pdf>

- [19] Muller, J.-M., Brisebarre, N., Dinechin, F., Jeannerod, C.-P., Lefevre, V., Melquiond, G., Revol, N., Stehle, D., Torres, S.: Handbook of Floating-Point Arithmetic, (2010). <https://doi.org/10.1007/978-0-8176-4705-6>
- [20] Karp, A.H., Markstein, P.: High-precision division and square root. ACM Trans. Math. Softw. **23**(4), 561–589 (1997). <https://doi.org/10.1145/279232.279237>